Luminescence kinetics of Yb^{2+} in NaCl

Taiju Tsuboi
Faculty of Engineering, Kyoto Sangyo University, Kamigamo, Kyoto 603, Japan

Donald S. McClure and Wing C. Wong
Department of Chemistry, Princeton University, Princeton, New Jersey 08544

(Received 3 September 1992; revised manuscript received 2 February 1993)

The lifetime of luminescence in NaCl:Yb^{2+} crystals has been investigated using a streak-camera method. Two emission bands peaking at 400 and 432 nm (called bands I and II, respectively) are observed. In addition to a long lifetime of more than 0.3 ms previously observed for band II, it was observed that band I has a short lifetime of less than 3 μs and the lifetime decreases with increasing temperature, reaching a short lifetime of 15 ns at 290 K. A kinetic analysis of the lifetimes and intensities of the bands in terms of three rate constants was made. The temperature dependence of the nonradiative rate constant was shown to be well reproduced by multiple-phonon-decay formulas.

I. INTRODUCTION

The Yb^{2+} ion in cubic crystals has a $4f^{14}\,{}^1A_{1g}$ ground term and all of its lower excited states belong to the $4f^{13}5d$ configuration.[1] The allowed transitions from the ground state end in one of the 18 T_{1u} states. The lowest atomic term is $^3P_2$, which becomes E_u and T_{2u}. These latter two states are separated by only a few hundred cm^{-1} and are the lowest ones in the manifold. The next higher state is one of the T_{1u} states about 2000-cm^{-1} higher. The experimental and calculated spectra of $SrCl_2$:Yb^{2+} have been compared in detail and it was shown that crystal-field parameters can be chosen such that energies and intensities of the transitions to the 18 T_{1u} states are well explained.[1] Similar good results were obtained for NaCl:Yb^{2+} where there must be a Na^+ vacancy for charge compensation, showing that the asymmetry in the environment of the Yb^{2+} ion has little effect on its spectrum.[2]

Two luminescence bands are produced by the excitation in the Yb^{2+} absorption bands in NaCl crystals.[2] One (named band I) has a peak near 400 nm, while the other (band II) has a peak near 435 nm. Band I is much weaker than band II at 300 K, but, as temperature is lowered, it is enhanced, whereas band II is drastically reduced in intensity. Band I has a mirror-image relationship to the lowest electric-dipole-allowed absorption band (called A band).[2] From these results, band I has been assigned to the allowed transition from the lowest T_{1u} ($4f^{13}5d$) level to A_{1g} ($4f^{14}$) level, while band II is assigned to the forbidden transitions from the lowest excited states produced by the $4f^{13}5d$ configuration, T_{2u} and E_u, to the A_{1g} ground state[2] (Fig. 1). The same assignment has been made for two Yb^{2+} luminescence bands with a peak around 377 nm (called band I) and a peak around 405 nm (band II) observed in $SrCl_2$ crystals.[3]

The luminescence-lifetime measurement is useful to check the previous assignment for band I and II and to clarify the luminescence processes in the two bands. Previously the lifetime of band II was measured: The lifetime obtained is 260 μs at 300 K and 800 μs at 100 K.[2] However, the lifetime of band I was not measured because it is too fast to be measured with a flash lamp of 4-μs pulse width. This work was initially undertaken to confirm the fast decay of band I in NaCl:Yb^{2+} and to examine what kind of process is involved in the fast decay.

II. EXPERIMENTAL PROCEDURE AND RESULTS

Single crystals of NaCl:Yb^{2+} (0.01 mol % in the melt) were excited by a Molectron UV14 N_2 laser. The crystals

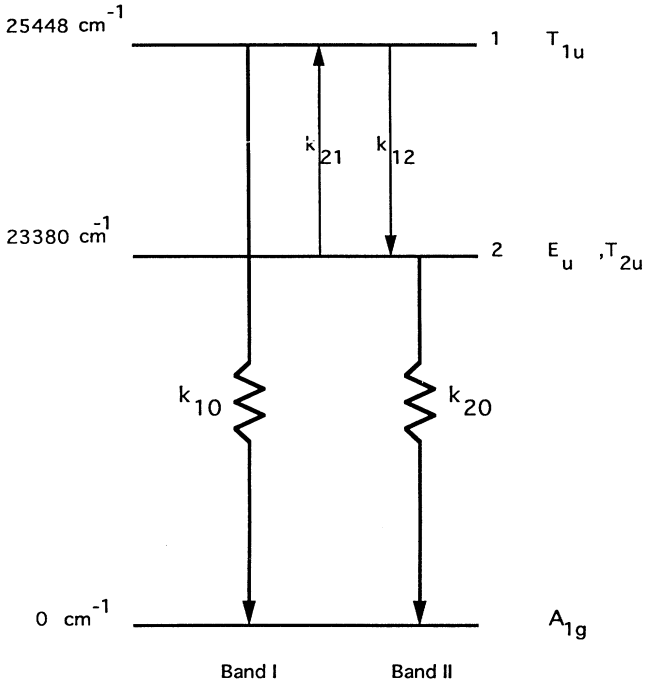

FIG. 1. Energy level diagram of Yb^{2+} showing rate constants.

were heated at 500 °C for 30 min and quenched to room temperature on a copper plate immediately before the measurement. The pulse width of the laser is 4 ns, and its peak power is 425 kW. The crystal luminescence was collimated, from the direction perpendicular to the exciting light, to an entrance slit of a Jobin-Yvon HR 320 polychromator where a ruled grating (size: 68×68 mm) with a groove density of 100 g/mm and a blaze wavelength of 450 nm is installed. The exit slit width was fixed to be 15 mm. The luminescence intensity was detected by a Hamamatsu Photonics C2830 streak camera attached with a Peltier-element-cooled charge-coupled device photodetector. It was possible to synchronize the laser pulse with the streak sweep within the jitter of less than 2 ns. The luminescence decay and time-resolved spectrum were obtained using a Hamamatsu Photonics Temporal Analysis computer system.

NaCl:Yb^{2+} has several absorption bands due to the electronic transitions in the Yb^{2+} ion, called $A,B,C...$ bands in order of increasing energy. The broad A band is located at 395–360 nm and the B band at 346–330 nm.[2] Therefore the N_2 laser emitting at $\lambda=337.1$ nm excites the high-energy side of the B band. Two luminescence bands with a peak at 400 nm (band I) and at 432 nm (band II) are produced, in agreement with the previous result obtained by the excitation of the A band. Luminescence spectra at a series of temperatures are shown in Fig. 2. It is seen that band II is present even at 20 K and that it increases as band I decreases with rising temperature.

A single luminescence decay curve was observed in the semilog plot for each of the bands I and II at various temperatures between 15 and 300 K. The lifetimes of the two bands are quite different from each other: For example, band I has a lifetime of at most 3 μs at 50 K, while band II has a long lifetime of 1860 μs at 15 K and 282 μs at 300 K, in agreement with previous results within experimental error. A typical decay curve is shown in Fig. 3(a) for band I and in Fig. 3(b) for band II. Three-dimensional time-resolved luminescence spectra are shown in Fig. 4. Band I decays quickly as seen in Fig. 4(a), while band II decays very slowly as seen in Fig. 4(b). Neither peak shift nor splitting are observed for either of the two bands as time evolves, indicating that only two luminescence bands, bands I and II, are produced by the excitation in the Yb^{2+} absorption band.

Band II of $SrCl_2$:Yb^{2+} has been observed to be composed of two components: The fast component is 50 (250) μs and the slow one is 520 (1300) μs at 300 (85) K.[3] We tried to find two such components in band II of NaCl:Yb^{2+} at various temperatures between 17 and 300 K, but only one component was observed as seen in Fig. 3(b).

In Fig. 5, $\log_{10}(1/\tau_I)$ vs temperature and in Fig. 6(b), $1/\tau_2$ vs temperature are plotted, where τ_I and τ_2 represent the lifetimes of band I and II, respectively. The marked temperature dependence of band I is due to the nonradiative transition between level I and level II. Radiative transition between level I and level II is not expected to be significant, since it is only magnetic dipole

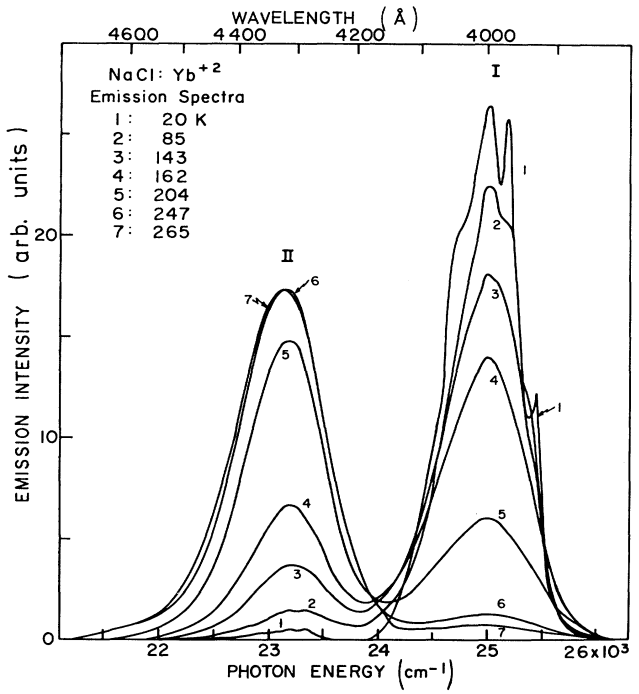

FIG. 2. Luminescence spectra of NaCl:Yb^{2+} at a series of temperatures.

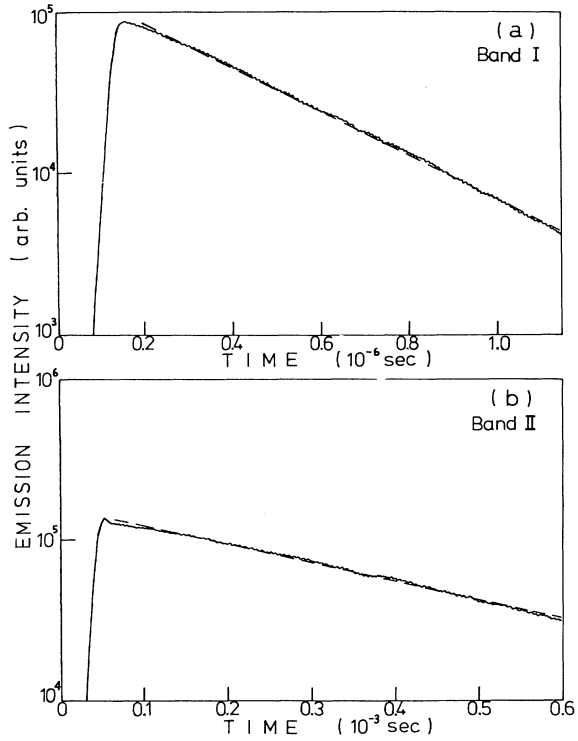

FIG. 3. Decay process in a semilog plot for (a) 400-nm emission band (band I) and (b) 430-nm emission band (band II) at 210 K.

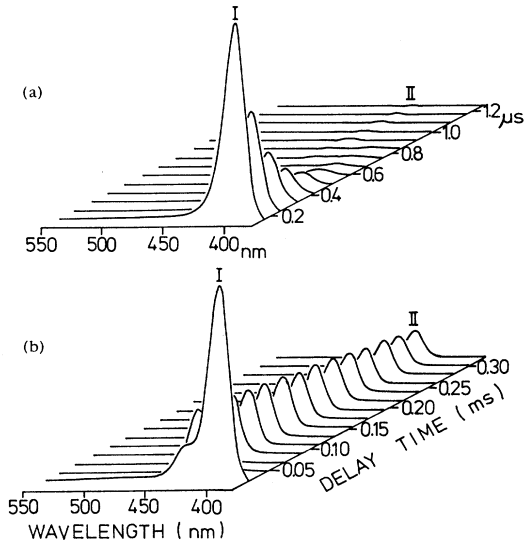

FIG. 4. Time-resolved spectra measured at 240 K in (a) 0.15–1.25 μs and (b) 0.03–0.35 ms after the N_2 laser excitation.

allowed. In Sec. III the three rate constants k_{10}, k_{20}, and k_{12} illustrated in Fig. 1 will be determined from the data and it will be seen that k_{12} has the strongest temperature dependence.

Table I shows the lifetime and intensity data upon which the analysis in Sec. III will be based. The intensity refers to the integrated area over time in terms of number of photons. The sum of the intensities is not exactly constant with temperature as it should be if the total quantum yield is unity, as was assumed in our previous publications; there is a decrease of about 28% in $I_{\rm I}+I_{\rm II}$ from low to high temperature. Whether this represents a decrease in total quantum yield or is an experimental error, we do not know.

III. DISCUSSION

The time dependencies of the populations of levels I and II can be analyzed by the kinetic equations,

$$-\frac{dN_{\rm I}}{dt}=k_{10}N_{\rm I}+k_{12}N_{\rm I}\ ,$$
$$-\frac{dN_{\rm II}}{dt}=-k_{12}N_{\rm I}+k_{20}N_{\rm II}\ , \tag{1}$$

where the rate constants are defined in Fig. 1. We assume $k_{21}=0$. With a population $N_{\rm II}(0)=0$ and $N_{\rm I}(0)\neq 0$ at $t=0$, we have

$$\frac{N_{\rm I}(t)}{N_{\rm I}(0)}=e^{-t/\tau_{\rm I}}\ ,$$
$$\frac{N_{\rm II}(t)}{N_{\rm I}(0)}=\frac{k_{12}}{k_{12}+k_{10}-k_{20}}(e^{-t/\tau_2}-e^{-t/\tau_{\rm I}})\ ,$$

where $\tau_{\rm I}=(k_{10}+k_{12})^{-1}$ and $\tau_2=k_{20}^{-1}$. From these formulas, both the temporal behavior of the two bands and their intensity relative to each other can be derived when the proper values of the parameters are inserted.

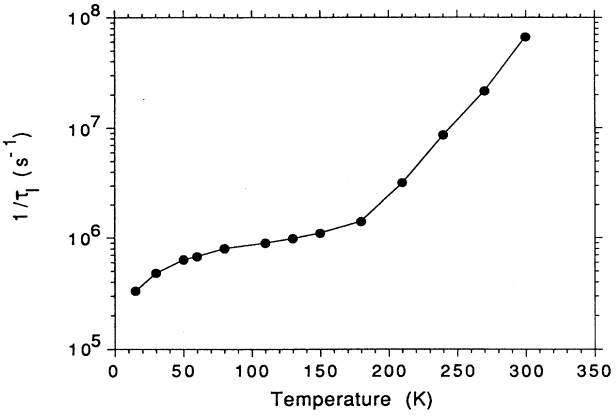

FIG. 5. $\log_{10}(1/\tau_{\rm I})$ vs temperature for band I.

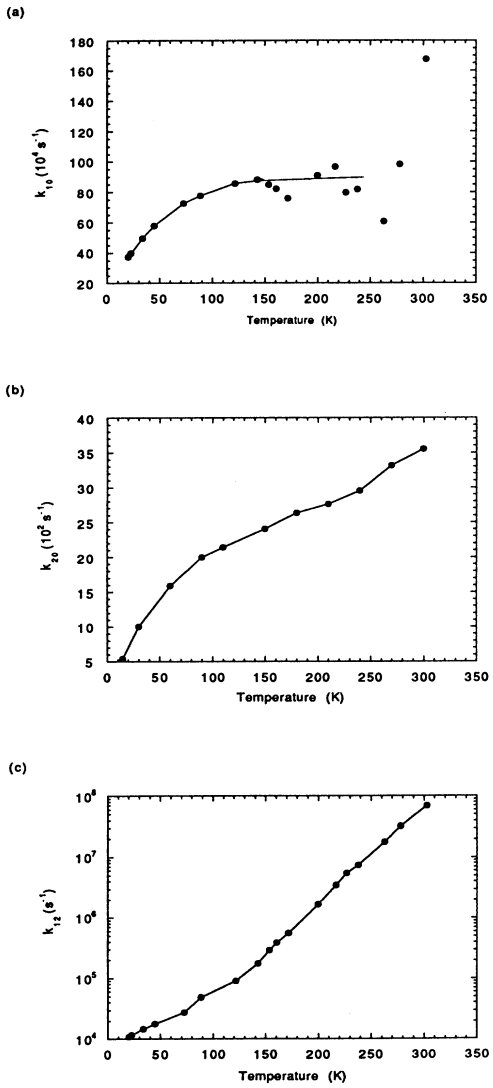

FIG. 6. (a) k_{10} vs T, (b) k_{20} vs T, and (c) semilog plot of k_{12} vs T.

TABLE I. Lifetime and intensity data for band I and band II from which k_{10}, k_{20}, and k_{12} are calculated.

(K)	Emission intensity I_I[a]	I_{II}[a]	I_I+I_{II}	Φ_{II}	k_{10}/k_{12}	$k_{10}+k_{12}$[b] (10^4 s^{-1})	k_{12} (10^4 s^{-1})	k_{10} (10^4 s^{-1})	k_{20}[c] (10^2 s^{-1})
20.4	1200	35.0	1240	0.0283	34.4	38.4	1.09	37.3	7.15
22.9	1200	35.0	1240	0.0283	34.4	40.9	1.16	39.7	7.87
34.0	1200	35.3	1240	0.0285	34.0	50.9	1.45	49.5	10.8
45.0	1190	36.6	1220	0.0299	32.4	59.4	1.78	57.7	13.2
73.0	1150	43.0	1190	0.0361	26.7	75.2	2.72	72.5	17.9
89.0	1120	69.7	1190	0.0585	16.1	82.3	4.81	77.5	19.7
122	1020	108	1130	0.0955	9.47	94.5	9.03	85.5	22.4
143	912	181	1090	0.166	5.03	106	17.5	88.1	23.7
154	794	271	1070	0.255	2.93	114	28.9	84.8	24.3
161	708	334	1040	0.320	2.12	121	38.7	82.0	24.7
172	631	465	1100	0.425	1.36	132	55.9	75.8	25.3
200	403	739	1140	0.647	0.546	258	167	90.9	27.0
217	229	819	1050	0.781	0.280	442	345	96.6	28.2
227	123	838	961	0.872	0.147	622	542	79.5	28.9
238	93	838	931	0.900	0.111	819	737	81.8	29.8
263	29	858	887	0.967	0.0341	1840	1780	60.6	32.0
278	26	858	884	0.971	0.0303	3340	3240	98.2	33.4
303	21	858	879	0.976	0.0243	7070	6900	170	35.9

[a]From integrated area.
[b]From interpolation of $(\tau_I)^{-1}$.
[c]From interpolation of $(\tau_2)^{-1}$.

The kinetic Eqs. (1) have not included any nonradiative process to the ground state, and we will derive the rate constants on the assumption that this is correct. The relative quantum yields given by Eqs. (1) are

$$\Phi_I=\frac{k_{10}}{k_{10}+k_{12}};\quad \Phi_{II}=\frac{k_{12}}{k_{10}+k_{12}}\ .$$

The relative intensities are the same as these quantum yields when the intensities are expressed in terms of photon yield. The rate constants derived from these and the lifetimes are given in Table I, and plotted in Fig. 6.

The values of $k_{10}(T)$ shown in Table I and Fig. 6 are calculated from $k_{10}=1/\tau_I-k_{12}$. The errors in using this relation are rather large above 150 K because k_{10} becomes the difference between two large numbers. It rises from 0.32×10^6 s^{-1} at 15 K to 0.86×10^6 s^{-1} at 150 K and then remains constant within the error limits.

The values of $k_{20}(T)=1/\tau_2$ are accurately known (see Table I). The data show a rise at low temperatures similar to k_{10}, but also a definite slow rise at higher temperature. The latter can be explained by a vibronic mechanism using $k(T)=k(0)\coth(hc\bar{\nu}/2kT)$ with $\bar{\nu}=288$ cm^{-1}. When this function is fitted to the highest temperature points and then subtracted from the data at all temperatures, a curve like that of $k_{10}(T)$ vs temperature is obtained, revealing a rapid increase in rate from 20 to 120 K. Band II is a symmetry-forbidden transition so that its temperature dependence is understood in terms of vibronic coupling. This seems to be true in spite of the presence of a charge compensating Na^+ vacancy, which could have reduced the symmetry and caused the transition to become allowed. The value 288-cm^{-1} is reasonable for a e_g stretching mode of the $YbCl_6$ octahedron, and it is this symmetry which would cause the emitting T_{2u} state to mix with T_{1u} states. The other component of the emitting level has E_u symmetry for which a t_{2g} mode would cause mixing with T_{1u} states. The t_{2g} mode is expected to have a much lower frequency.

Multiple-phonon nonradiative decay has been studied extensively theoretically.[4-11] While the trivalent rare-earth ions are treated in the regime of weak electron-phonon coupling, the divalent ytterbium ion has a relatively diffuse $5d$ electron which renders the coupling to be stronger, a situation not unlike the transition-metal ions. For simplicity, a one-dimensional configuration model is usually adopted. Based on the experimental results obtained, a comparison will be made for two of the theoretical methods.[12] The first one is based on the assumption that there is no displacement in the normal coordinates for the two states between which the radiationless decay is happening. Because of this, the harmonic phonon states can have transitions of only a single quantum. The multiple-phonon transition happens through a pth order perturbation approximation where p is the number of phonons involved. By considering an average phonon energy $\bar{\nu}$ (in cm^{-1}), the temperature dependence of a nonradiative process can be written as (Keil's formula):[4,5]

$$k_{12}(T)=k_{12}(0)(1+n)^p\ , \tag{2}$$

where $k_{12}(0)$ is the rate at 0 K and $n=[\exp(hc\bar{\nu}/kT)-1]^{-1}$, the average occupation number of the phonons.

Because both excited states are derived from a similar

electronic configuration, $4f^{13}5d$, the displacement in the potential surfaces should be small. It can be proved by noting that the estimated Huang-Rhys factors S are 2.5 and 1.5 for bands I and II, respectively. This gives an effective $S=0.13$ between the two states. Because of this small-S factor for the transition between the two excited states, it is not physically reasonable to expect a crossing of their potential surfaces at an energy low enough for an activated crossing process. We have fitted Eq. (2) to the data for k_{12} at and above 200 K. The parameters are $k_{12}(0)=13\,250$ s^{-1}, $p=16$, and $\bar{\nu}=185$ cm^{-1}, giving a sum of squared residuals of 0.0178. It fits well in the region above 120 K and approximately in the region below 120 K.

We also compared our data to the other model, which is the nonadiabatic Hamiltonian method. In this model, the Huang-Rhys factor S is nonzero. This makes the multiple-phonon transition allowed in the first order. Briefly, the Fermi golden rule is applied for the transition probability between the states with the matrix element of the nonradiative Hamiltonian left out in the Born-Oppenheimer approximation. Then the sum is obtained from the result of Huang and Rhys.[13]

Neglecting the $(p-1)$ and $(p-2)$ phonon processes, while taking the electron factor to be $e^{-S}S^p/p!$, the nonradiative decay rate can be written as

$$k_{12}(T)=k_{12}(0)e^{-2nS}p!S^{-p}[(n+1)/n]^{(p/2)} \times I_p[2S\sqrt{n(n+1)}]\ , \quad (3)$$

where I_p is the modified Bessel function of order p and $n=[\exp(hc\bar{\nu}/kT)-1]^{-1}$.

Again, the data at and above 200 K were chosen for the fitting. With $S=0.13$, the best fit based on the nonadiabatic Hamiltonian method is found at $k_{12}(0)=12\,250$ s^{-1}, $p=16.4$, and $\bar{\nu}=184$ cm^{-1} with a sum of squared residuals of 0.0171. The fitted curve is shown in Fig. 7. The parameters are not too different from the other model. In fact, Eq. (3) reduces to Eq. (2) as S approaches zero. We expect Eq. (3) to be more suitable to our data, since we have a nonzero S and indeed the fitting was slightly better when Eq. (3) was used.

The fitting of the temperature dependence by the two models above may or may not be physically significant. In our previous publication[2] we fitted the data $I_I/I_{II}=k_{10}/k_{12}$ to the Keil model using the spectroscopically observed value of $\bar{\nu}=210$ cm^{-1} and $p=16$. Now with the measured values of k_{10} we are able to do a more complete analysis resulting in $\bar{\nu}=184$ cm^{-1} and $p=16.4$. This value of p gives the correct temperature dependence, but $p\cdot hc\bar{\nu}$ is larger than the observed ΔE of 2068 cm^{-1}.

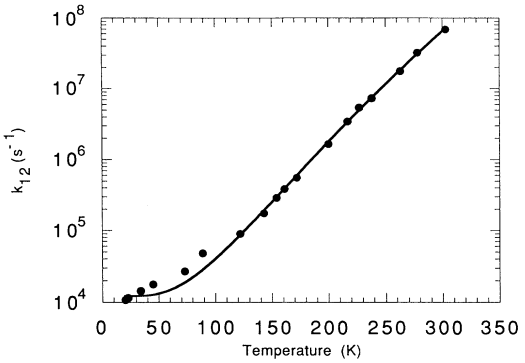

FIG. 7. Fitted curve for k_{12} vs T in the nonadiabatic Hamiltonian method [Eq. (3)] $k_{12}(T)=k_{12}(0)e^{-2nS}p!S^{-p}[(n+1)/n]^{(p/2)}I_p[2S\sqrt{n(n+1)}]$, with $k_{12}(0)=12\,250$ s^{-1}, $p=16.4$, $\bar{\nu}=184$ cm^{-1}, and $S=0.13$.

A smaller p value of 11.2 with $\bar{\nu}=184$ cm^{-1} would fit the gap but would give too low a temperature dependence. The average mode frequency of 184 cm^{-1} corresponds to the major peak in the density of phonon states of NaCl, and is thus physically reasonable. The spectroscopically observed frequency interval of about 210 cm^{-1} is in a sparse region of the phonon density of states vs frequency and is probably a pseudolocal mode involving the chloride ions near the charge compensating Na^+ vacancy. Perhaps it is physically reasonable that the 184-cm^{-1} lattice mode rather than the 210-cm^{-1} local mode carries away the energy in the decay process.

All three rate constants show a rapid rise from 20 up to about 120 K. k_{10} appears to level off above 120 K; k_{20}, as we showed above, also levels off if the vibronic intensification is accounted for. Both of them increased by about a factor of 2 from 20 to 120 K. k_{12} lies above the multiple-phonon curve (Fig. 7) up to about 120 K. Therefore, the rapid rise is common to all three of the rate constants. The only common factor we can think of which could explain this is a change in the environment with rising temperature, perhaps associated with the nearby charge compensating Na^+ vacancy.

ACKNOWLEDGMENTS

The present work was supported by a Grant-in-Aid from the Japanese Ministry of Education and Science. We thank Dr. P. Silfsten for his assistance in the luminescence-lifetime measurement at the early stage of the present study. Work at Princeton was aided by the National Science Foundation Grant No. CHE-8806365.

[1]T. S. Piper, J. P. Brown, and D. S. McClure, J. Chem. Phys. **46**, 1353 (1967).

[2]T. Tsuboi, H. Witzke, and D. S. McClure, J. Lumin. **24/25**, 305 (1981).

[3]H. Witzke, D. S. McClure, and B. Mitchell, in *Luminescence of Crystals, Molecules and Solutions,* edited by F. E. Williams (Plenum, New York, 1973), p. 598.

[4]A. Keil, in *Quantum Electronics,* edited by P. Grivet and N. Bloembergen (Columbia University Press, New York, 1964), Vol. 1, p. 765.

[5]F. Auzel, in *Luminescence of Inorganic Solids,* edited by B. DiBartolo (Plenum, New York, 1978), p. 67.

[6]L. A. Riseberg and H. W. Moos, Phys. Rev. **174**, 429 (1968).

[7]H. W. Moos. J. Lumin. **1/2**, 106 (1970).

[8]T. Miyakawa and D. L. Dexter, Phys. Rev. B **1**, 2691 (1970).
[9]F. K. Fong, S. L. Naberhuis, and M. M. Miller, J. Chem. Phys. **56**, 4020 (1972).
[10]W. E. Hagston and J. E. Lowther, Physica **70**, 40 (1973).
[11]M. D. Sturge, Phys. Rev. B **8**, 6 (1973).
[12]F. Auzel, in *Radiationless Processes,* Vol. 62 of *NATO Advanced Study Institutes Series B: Physics,* edited by B. Di Bartolo (Plenum, New York, 1979), pp. 213–286.
[13]K. Huang and A. Rhys, Proc. R. Soc. (London) Ser. A **204**, 406 (1950).